THE JOURNAL OF PHYSICAL CHEMISTRY C

Article

Halide-Gated Molecular Release from Nanoporous Gold Thin Films

Ozge Polat, and Erkin Seker

J. Phys. Chem. C, **Just Accepted Manuscript** • DOI: 10.1021/acs.jpcc.5b06959 • Publication Date (Web): 08 Sep 2015

ACS Publications

The Journal of Physical Chemistry C is published by the American Chemical Society. 1155 Sixteenth Street N.W., Washington, DC 20036

Halide-Gated Molecular Release from Nanoporous Gold Thin Films

Ozge Polat[a], Erkin Seker[b*]

[a]Department of Chemical Engineering and Materials Science

[b]Department of Electrical and Computer Engineering

University of California - Davis, Davis, CA 95616, USA

*Corresponding author: eseker@ucdavis.edu

ABSTRACT

Nanoporous materials have attracted significant attention as drug delivery platforms, in which interfacial phenomena are often more influential than fluid mechanics in defining molecular loading capacity and release kinetics. This study employs nanoporous gold (np-Au) as a model material system to investigate physical mechanisms of molecular release of fluorescein (a small molecule drug surrogate) from the sub-micron-thick np-Au coatings. Specifically, the study reveals an interfacial mechanism where halide ion-gold surface interactions dictate the loading capacity and release kinetics of fluorescein. We systematically study the effect of halide concentration and species on release kinetics from sputter-deposited np-Au films with a combination of quantitative electron microscopy, fluorospectrometry, and electrochemical surface characterization techniques. The results suggest that the interplay of halide-gold interaction probability and affinity determine the nature of release kinetics. The former mechanism plays a more dominant role at higher ionic strengths, while the latter is more important at lower ionic strengths. This interfacial phenomenon is further complemented by functionalizing the np-Au with self-assembled monolayers (SAMs) of alkane-thiols for modulating gold surface-halide affinity and consequently the molecular release kinetics.

INTRODUCTION

There has been a surge of interest in novel material systems for drug delivery platforms with the overarching goal of controlled and targeted delivery of pharmaceuticals.[1, 2] Advancements in materials with nanometer-scale features and their application to biomedical sciences resulted in a variety of biomaterials for cancer therapeutics, vascular stents, and neurological applications.[2, 3] To that end, nanostructured materials such as porous silicon[4, 5], anodic nanoporous alumina,[1, 3] metal oxide nanotubes,[1, 2, 6, 7] carbon nanotubes,[8-10] and polymers[11, 12] have become popular in the recent years as drug delivery platforms due to their tunable porosity and pore morphology for controlling release kinetics. Nanoporous gold is an emerging material that attracted significant attention for its unusual catalytic and optical performance,[13-16] as well as its versatility in studying structure-property relationships for numerous applications.[17-21] Np-Au is typically synthesized by selective dissolution of silver from a silver-rich gold-silver alloy, where surface diffusion of gold atoms lead to a bicontinuous open-pore morphology.[22] This process, also known as *dealloying*, produces ~70% porosity and pore/ligament sizes in the range of tenths of nanometers. Variety of post-processing techniques, most popularly thermal treatment, can be used to coarsen the pores/ligaments as much as several microns while still maintaining a self-similar morphology.[23-26] The facile synthesis and tunable morphology, combined with compatibility with conventional microfabrication processes, high electrical conductivity[26], well-established gold-thiol linker chemistry, and biocompatibility easily explain its popularity as a material system.[27] During the last few years, these attributes led to np-Au's use flourishing in biomedical applications, including biosensors,[28-30] neural electrodes,[31, 32] and drug eluting coatings.[33] Our previous mechanistic study of molecular release from np-Au thin films revealed that the interplay of surface area and pore morphology dictate loading capacity and release kinetics of small molecule release.[33] More specifically, the molecular release from np-Au is due to desorption of molecules adsorbed on the pore walls and their outflux through the porous

network. Here, we focus on the effect of ionic ambient on the release, specifically focusing on the halide-gold surface interactions that dictate the release kinetics.

MATERIALS AND METHODS

Chemicals and Materials

The substrates (12 mm x 24 mm glass coverslips) to be coated with np-Au were purchased from Electron Microscopy Sciences. Chrome, gold, and silver targets for deposition were purchased from Kurt J. Lesker. Polydimethylsiloxane (PDMS) elastomer sheets used for stencil masks were obtained from B & J rubber products. Fluorescein sodium salt, sodium hydroxide, nitric acid (70%), sulfuric acid, sodium fluoride, sodium chloride, sodium bromide, sodium iodide, and 1-propanethiol were all purchased from Sigma Aldrich. Dulbecco`s phosphate-buffered saline (no calcium, no magnesium) (1x-DPBS) was purchased from Life Technologies.

Fabrication and Characterization of np-Au Samples

The np-Au sample preparation has been described in detail previously.[27, 33, 34] Briefly, laser-cut PDMS stencil masks were used in order to create 3 mm x 3 mm square patterns of np-Au on the glass coverslips. The stencil mask-screened glass coverslips were loaded into a sputtering instrument (Kurt J. Lesker) to be coated with 160 nm of chrome adhesion layer and 80 nm of gold seed layer. Without breaking the vacuum, the samples were successively coated by 600 seconds of co-sputter of gold and silver in order to create a silver rich gold-silver alloy. After the deposition, the samples were dealloyed by immersion in 70% nitric acid at 55 °C to create the intended np-Au thin film. Each glass coverslip was then manually cut with a diamond scriber to produce the final samples (i.e., 4 mm x 6 mm glass chips with a 3 mm x 3 mm np-Au pattern). Prior to any experimental processing, the np-Au chips were oxygen plasma-cleaned for 40 s at 10 W in order to increase the hydrophilicity of the surface.[34] The film thickness and pore morphology were determined with a scanning electron microscope (SEM, FEI Nova

NanoSEM430). ImageJ and a custom MATLAB script were used to analyze top-view SEM images in order to determine pore area and ligament size.[31] Energy dispersive X-ray spectroscopy (EDS, Oxford Inca Energy) was used to determine the elemental compositions of the films. Electrochemical characterization was used to calculate the effective surface areas of the samples. Briefly, cyclic voltammograms in 50 mM sulfuric acid were recorded with a scan rate of 50 mV/s by a potentiostat (Gamry Reference 600) in combination with a Teflon electrochemical cell, Ag/AgCl reference electrode, and platinum counter electrode. The area under the gold oxide (AuO) reduction peak (potentials between 615 mV and 1.045 V) was integrated to calculate the charge involved in the reaction. Corresponding effective surface area of np-Au chips were finally determined with 450 $\mu C/cm^2$ as specific charge of gold surface and the surface enhancement factor was calculated by taking the ratio of effective surface area of np-Au to the effective surface area of planar gold (pl-Au).[35]

Loading and Molecular Release Quantification

Fluorescein sodium was used as a small molecule drug surrogate.[33, 36, 37] Np-Au chips were incubated for 16 hours inside a 10 mM fluorescein sodium salt solution in a 0.25 mL microcentrifuge tube at room temperature without exposure to ambient light. Preliminary studies indicated that a loading isotherm is reached between 1 mM to 10 mM. After incubation, fluorescein solution was aspirated and samples were rinsed three times with deionized (DI) water inside the incubation tubes. After aspiration and rinsing, each chip was dipped into a 1L-beaker filled with DI water for 10 seconds in order to wash off any residual fluorescein molecules from the outside surfaces of the chips. After this step, each chip was placed inside a new microcentrifuge tube containing the *elution medium* of interest. In this work, DI water, 1x-DPBS, as well as NaCl, NaF, NaBr, and NaI at varying concentrations were used as elution media. The release profile of each chip was monitored by sampling the elution media at specific time points and quantifying its fluorescence intensity (emission at λ=515 nm) with a

fluorospectrometer (NanoDrop 3300). Prior to each fluorescence measurement, 10 µL-sampled solution from the elution tube was mixed with 10 µL of 50 mM NaOH to increase fluorescence intensity.[33, 38] Loading capacity represents the cumulative mass released, which is determined as the average molecular mass that reached steady state. Fractional release is calculated by normalizing the mass released at each time point to the final mass released. Unless otherwise indicated, the plotted data points and error bars represent respectively the averages and standard errors of measurements from at least three different samples.

RESULTS AND DISCUSSION

The goal of this work was to study the effect of elution media constituents on fluorescein release (i.e., loading capacity and release kinetics) from np-Au chips (Figure 1).

Sample Characterization

The np-Au samples (3 mm x 3 mm square patterns of np-Au on the glass coverslips) were fabricated by sputtering a 600 nm-thick gold-silver alloy and dealloying them in nitric acid, which created a network of gold ligaments surrounded by inter-connected pores (Figure 1A and 1B). The elemental composition of the precursor alloy, as determined by EDS, was 35%:65% (Au:Ag, atomic percent) and the residual silver composition in np-Au films after dealloying was 3-5%.[27] The image analysis revealed a unimodal pore morphology (Figure S1) with typical pore diameters of 10 to 100 nm (extracted from the pore areas by approximating the pore shape as circular for simplicity) and an average ligament width of 56.9±1.6 nm. Minor hairline cracks, due to the release of tensile stress during dealloying,[39] were also observed in the np-Au films and their influence on molecular release was reported in our previous work.[33] The cyclic voltammetric characterization of np-Au thin films revealed an effective surface area of 7.32±0.59 cm^2, which constitutes an enhancement of 12.5 times over a pl-Au surface with the same

footprint (Figure 1C). We previously reported that this large effective surface area plays an important role in the release kinetics and loading capacity.[33]

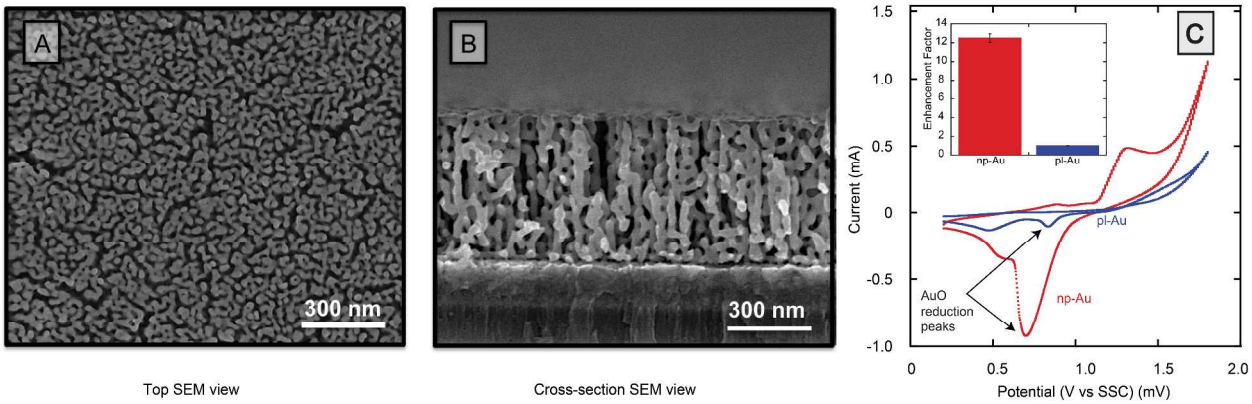

Figure 1. Top-view (A) and cross-section (B) of a 600 nm-thick np-Au sample that is representative of those used in the experiments. (C) Cyclic voltammograms of np-Au thin film and a pl-Au counterpart with the same footprint, indicating the 12.5-fold surface area enhancement.

Sustained versus Immediate Release Phenomenon

Our previous work focused on the effect of np-Au film thickness and pore morphology on fluorescein release into DI water.[33] The 600 nm-thick np-Au films used in this study displayed a sustained release of 0.13±0.01 μg of fluorescein up to two weeks. Surprisingly, when samples (prepared and loaded with the identical procedure) were placed in an elution medium of 1x-DPBS instead of DI water, almost twice as much fluorescein (0.25±0.02 μg) was released (Figure 2). Perhaps more strikingly, the fluorescein release kinetics into DPBS was significantly different than for DI water, with almost an immediate release of the molecular cargo.

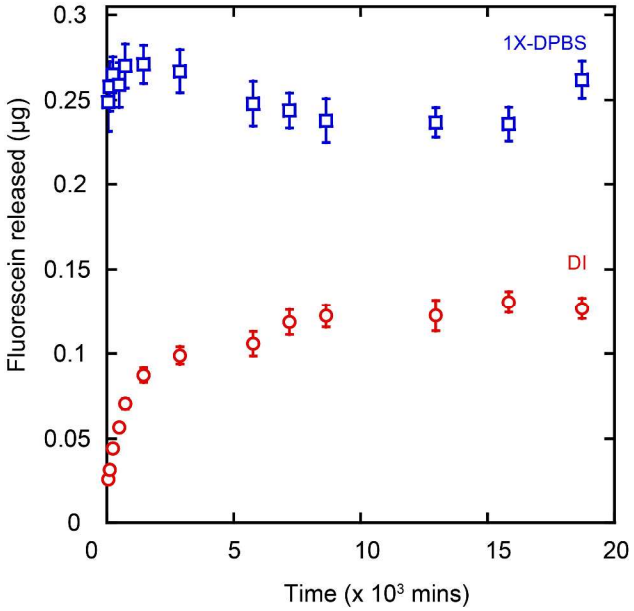

Figure 2. Release profile of fluorescein from identically-loaded np-Au samples into DI water and 1x-DPBS. For the case of DPBS, the release kinetics was significantly increased and twice as much fluorescein was delivered into the elution medium in comparison to the case for DI water.

The drastic difference in the release profiles was attributed to the constituents of DPBS and this motivated the subsequent studies. 1x-DPBS is composed of 2.67 mM potassium chloride, 1.47 mM potassium phosphate monobasic, 8.06 mM sodium phosphate dibasic and 136.9 mM sodium chloride, indicating the dominance of chloride ions in the elution medium. First, in order to differentiate between the possible effects of the alkaline component (i.e., Na^+ vs. K^+), we conducted a release experiment with 0.1 mM NaCl and KCl as the elution media. No significant difference was observed between the sodium and potassium in terms of release kinetics (Figure S2), and the difference in loading capacity was negligible (Figure S2 inset). Therefore, NaCl was selected for the further experiments to investigate the effect of the anion, since sodium and chloride are the principal ions in extracellular fluid contributing to the charge and concentration balance across cell membranes.[40, 41]

Molecular release from np-Au is a combination of two mechanisms: desorption of surface-adsorbed molecules onto pore walls and transport of fluorescein molecules through the porous volume.[33] It is illustrative to estimate the time it would take for fluorescein molecules to vacate the np-Au network if the release was purely dominated by Fickian diffusion. In this case, a simple calculation of diffusion length ($x \approx \sqrt{(Dt)}$[33]) equated to the length of an average porous channel through film thickness (product of film thickness and tortuosity of 3.2±0.2[42]) of 1920 nm, indicates an extremely short duration of 8 ms. This contradicts with the sustained release duration of hours to weeks,[33] underlining the importance of surface-mediated mechanisms in prolonging molecular release duration.[1, 2] This also illuminates the putative mechanisms as to how chloride ions might be accelerating the fluorescein release. The affinity of chloride ions to gold is well known and it is plausible that chloride ions in the elution medium can replace physio-adsorbed fluorescein molecules.[43-47] We therefore hypothesized that in the presence of halides, the release kinetics and loading capacity are dictated by halide-gold interactions. This process can be deconstructed into two key mechanisms: (1) Probability of halide-ions interacting with the gold surface and (2) binding affinity of a halide upon collision with the gold surface. We now focus on experiments to investigate these two complementary mechanisms in describing concentration and halide-species dependence.

Ionic Strength-Dependent Release Process

As the ionic strength of the elution medium (i.e., concentration of chloride) increases, the probability of a chloride ion interacting with gold surface increases (Mechanism 1 described above). This, in turn, translates into a larger number of ion-surface interactions accumulating within a unit time window for the cases of higher ionic strength. Figure 3A validates this notion, where the release kinetics became faster as the NaCl concentration in elution medium increased. At the highest concentration of 100 mM (approaching chloride concentration in

DPBS), the fractional release indeed became instantaneous similar to the case with DPBS (Figure 2). The loading capacities for different NaCl concentrations and DI water normalized to the loading capacity for 100 mM revealed less than 40% change in loading capacity. This suggests that a kinetic equilibrium between adsorption and desorption rates of chloride and fluorescein ions with the gold surface might dictate the ultimate loading capacity. Put another way, given that both the chloride and fluorescein ions can displace each other, at a higher chloride concentration, it is expected that a larger proportion of these interactions would involve chloride displacing fluorescein. The net result would be that a larger number of fluorescein molecules would desorb and exit the porous network (readily quantified as fluorescence intensity of the elution medium), thereby leading to a higher loading capacity. It is important to consider the role of the aforementioned Mechanism 2 in the release process, where chloride-gold binding affinity is larger than that of fluorescein-gold. For the former the main intermolecular force is deemed as covalent interactions,[45-48] while for the latter Van der Waals forces should be prevalent, as fluorescein is not composed of atoms with known gold affinity (such as halides and sulfur) or surface charge of gold is not positive enough to yield a strong electrostatic interaction with negatively-charged fluorescein. This, in effect, biases the equilibrium towards chloride adsorption and consequent fluorescein desorption. Accordingly, a loading capacity isotherm with respect to chloride concentration was quickly reached (Figure 3A inset), which supports that the binding affinity of chloride dominates over that of fluorescein.

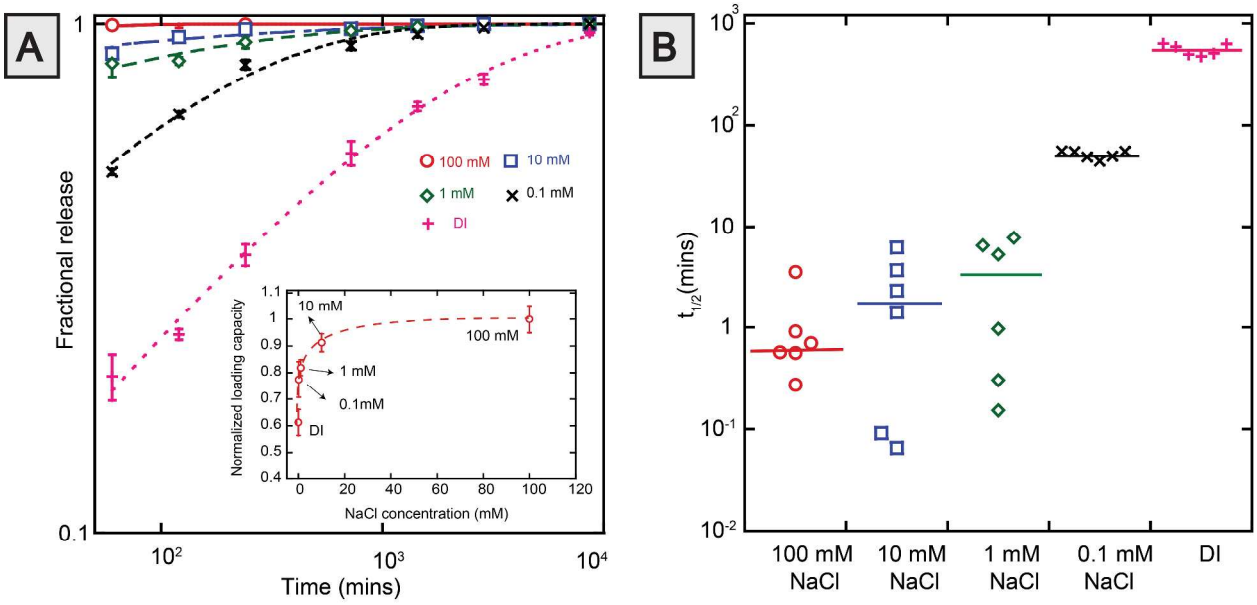

Figure 3. (A) Release profile of fluorescein into DI water and elution media with 0.1 mM, 1 mM, 10 mM, and 100 mM NaCl. Inset: Normalized loading capacity (to loading capacity at 100 mM) versus NaCl concentration. (Dashed lines in the inset are visual guides only) (B) Release half-life versus NaCl concentration. (Solid lines indicate the median of the corresponding data points). Higher NaCl concentration accelerates the fluorescein release from np-Au films, even though the loading capacity quickly reaches a maximum with increasing NaCl concentration.

Another measure of a release process is the release rate, where the time it takes to release 50% of the loading capacity (half-life, $t_{½}$) is a conventional metric. We previously employed a curve-fit analysis proposed by Papadopoulou *et al.* that uses Weibull distribution function for extracting information about the release mechanisms.[49] This analysis allows for determining release half-life and provides insight into the geometry of the drug-eluting material.[33] In this approach, fractional release data (Figure 3A) is fitted into:

$$\left(\frac{M_t}{M_\infty} = 1 - exp\left(-at^b\right)\right)$$

where M_t and M_∞ are the cumulative amounts of release at a specific time point t and at the end of the release respectively. The curve-fit parameters a and b provide insight into possible

release mechanisms.[49] As mentioned in the previous work, kinetics of release from np-Au, where values for *b* were smaller than 0.69,[33] indicate molecular release geometries with increasing disorder of the porous network[49]. The half-lives were calculated by setting $\frac{M_t}{M_\infty} = 0.50$. The release half-life for the 100 mM NaCl case was on the order of one minute, while the half-life was approximately an hour for the 0.1 mM NaCl (Figure 3B). The inverse proportionality between half-life and NaCl concentration can again be explained by the combined effects of chloride-gold interaction frequency (Mechanism 1) and chloride-gold binding affinity (Mechanism 2). As fluorescein molecules desorb upon chloride adsorption to gold, they migrate out of np-Au due to the steep concentration gradient between fluorescein within the np-Au film and the elution medium. Together with faster saturation of the gold surface at increased chloride concentration (thus more fluorescein desorption within unit time), it is suspected that fluorescein-surface affinity also diminishes, thereby reducing surface interaction-hindered transport of fluorescein (as for the case of DI water).

In summary, the release process (i.e., kinetics and loading capacity) is mainly dictated by Mechanisms 2 in lower ionic strengths; where for a reduced probability of a halide interacting with the pore wall, the likelihood of a halide molecule permanently binding onto the surface upon collision is the limiting-factor. On the other hand, for higher ionic strengths; where the probability of halide-surface interaction is very high, the proportion of adsorbed halide per unit area and unit time is enhanced and Mechanism 1 becomes more dominant.

Halide Species-Dependent Release Process

To specifically investigate the effect of binding affinity, we investigated different halide species. In the light of the notion that Mechanism 2 (binding affinity) is the factor that shapes the release process, we used low concentrations (0.1 mM) of sodium salt solutions of different halides (i.e.,

fluoride, chloride, bromide and iodide). Halides are known to create adlayers on metallic electrode surfaces and the degree of specific adsorption to gold surface increases in a fashion of $F^-<Cl^-<Br^-<I^-$.[44, 45, 48] It is therefore expected that more fluorescein should be displaced from the surface in a unit time in the presence of halides with high gold affinity. In agreement with this hypothesis, the observed release rate was higher for halides with higher gold affinity (Figure 4).

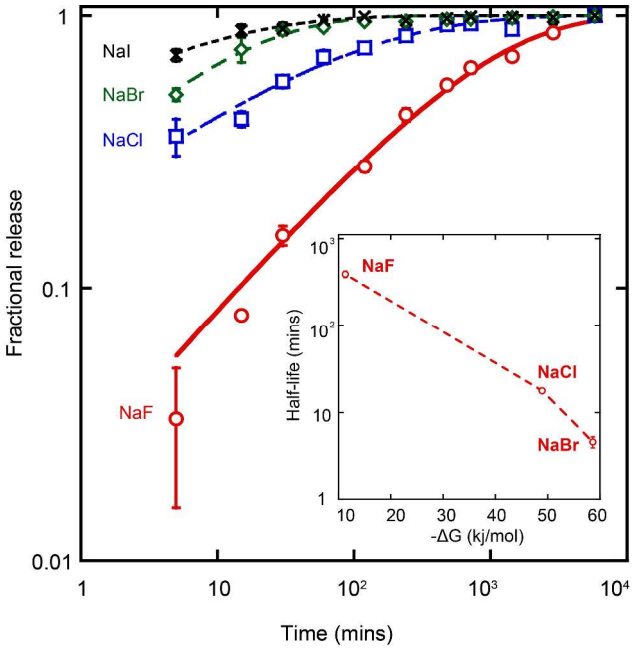

Figure 4. Release profile of fluorescein into 0.1 mM elution media of NaF, NaCl, NaBr, and NaI. Inset: Corresponding half-lives of the release versus free energy of adsorption of halides onto gold (Theoretical calculation values from Bodé *et al.*[50])

More specifically, the slowest release was observed for the elution medium of NaF, which can be explained by the fluoride having the lowest affinity to the gold surface,[45] where the kinetic equilibrium between adsorption and desorption of fluoride and fluorescein onto the gold surface is not biased towards fluoride adsorption as was the case for chloride. The similarity between the release rates for Cl^-, Br^-, and I^- is likely due to the ionic strength of 0.1 mM still being high enough that Mechanism 1 contribution is not negligible. For providing further insight into the

relationship between the spontaneity of halide adsorption onto gold surface and the resultant release rate, we used free energy (ΔG) of adsorption of halides onto gold electrode obtained by theoretical calculations by Bodé *et al*. [50] (Figure 4 inset). The monotonic trend shows that halide adsorption becomes more favorable in the order of $F^-<Cl^-<Br^-$ [50, 51] with a corresponding decrease in the half-life of the release. It is worth mentioning that iodine is an established gold etchant and halide additives can modify np-Au morphology during dealloying.[52, 53] This highlights that the iodine-gold affinity is so high that it exhibits a chemical interaction and also suggests the possibility that halide-gated release may be influenced by halide-mediated restructuring (via enhanced gold surface diffusion[22]) of the gold surface[52]. In order to test this possibility, the morphology of a np-Au chip before and after a week-long DPBS soak was compared; however, there was no observable change in the morphology (Figure S3). Given that the presence of chloride has an immediate effect (minutes) on the release kinetics, the absence of any morphological change in DPBS after a week suggests that surface restructuring was not significant in our study.

Modulating Sensitivity of Release to Halides

For the np-Au platform, halides can be viewed as stimuli that trigger the rapid release of fluorescein cargo. While gated-release is of significant interest for stimuli-responsive platforms,[54-59] the sensitivity of molecular release from the np-Au network to halides constitutes a challenge for using np-Au in physiological conditions due to the halide abundance.[40, 41] Informed by the results revealing halide-gold interaction as the main driver of the release process, we hypothesized that SAMs onto the gold ligaments might dampen the degree of halide-surface interaction, therefore modulating the release processes. We leveraged the robust thiol-gold based linker chemistry to modify the np-Au samples with 1-propanethiol prior to loading them with fluorescein. This approach significantly reduced the sensitivity to halides, where the release kinetics in DI water and DPBS for SAM-modified np-Au samples remained

similar (Figure 5). It should be noted that the loading capacity for the SAM-modified np-Au also decreased, as the SAM layer likely reduced the fluorescein-surface affinity. With the availability of a large repertoire of functional thiols[60, 61] and the ability to iontophoretically load np-Au films[62], it should be possible to optimize the system to circumvent the reduced loading capacity and also to modulate the sensitivity to halides or molecular triggers for tuning the release rate.

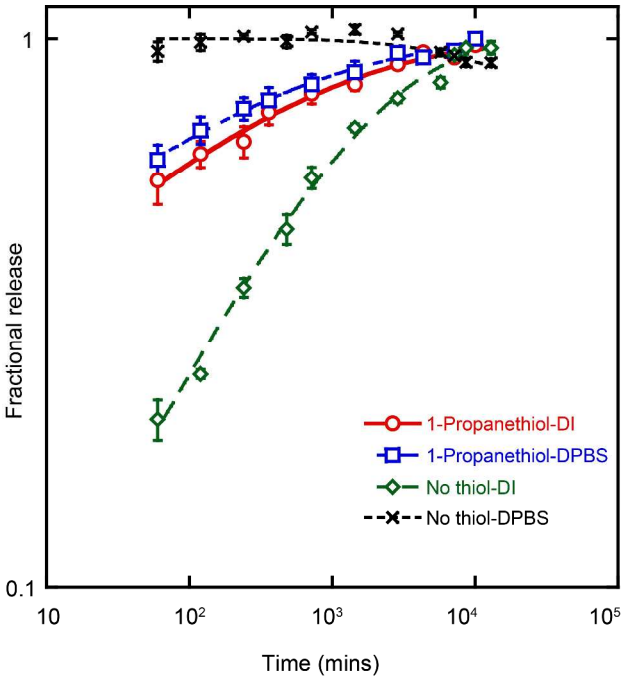

Figure 5. Release profile of fluorescein into DI water and DPBS from 1-propanethiol modified np-Au thin films versus non-modified np-Au thin films. The SAM modification reduces the sensitivity to halide presence in elution medium.

CONCLUSION

Motivated by the phenomenon of immediate molecular release from np-Au thin films in DPBS, we investigated the effect of halide concentration and species on release kinetics and loading capacity of fluorescein. The results revealed that the interplay of halide-gold interaction probability and affinity determined the nature of the observed release process. The former

mechanism played a more dominant role at higher ionic strengths, while the latter proved to be more important at lower ionic strengths. We finally demonstrated that this interaction can be modulated with the inclusion of thiol-based self-assembled monolayers. We anticipate that this work will not only pave the way to the development of tunable drug delivery tools but also inform the design of other platforms (e.g., electrochemical biosensors,[63] nanoparticle-based theranostics,[64] surface-enhanced Raman spectroscopy[65]), where gold is frequently used.

ACKNOWLEDGEMENT

We gratefully acknowledge the support from UC Lab Fees Research Program Award (12-LR-237197), UC Davis Research Investments in the Sciences & Engineering (RISE) Award, and National Science Foundation Awards (CBET-1512745 and CBET&DMR-1454426). We also thank Profs. Atul Parikh (UC Davis) and Arne Wittstock (University of Bremen) for discussions on molecule-surface interactions, Prof. Tingrui Pan (UC Davis) for his help in stencil mask preparation, and Dr. Ling Wang (UC Davis) for his help in pore morphology analysis.

Supporting Information. Pore size distribution of the nanoporous gold samples, effect of cationic species on molecular release, and effect of halides on surface reconstruction. This material is available free of charge via the Internet at http://pubs.acs.org.

REFERENCES

(1) Gultepe, E.; Nagesha, D.; Sridhar, S.; Amiji, M., Nanoporous Inorganic Membranes or Coatings for Sustained Drug Delivery in Implantable Devices. *Adv. Drug Del. Rev.* **2010**, *62*, 305-315.

(2) Aw, M. S.; Kurian, M.; Losic, D., Non-Eroding Drug-Releasing Implants with Ordered Nanoporous and Nanotubular Structures: Concepts for Controlling Drug Release. *Biomater. Sci.* **2014**, *2*, 10-34.

(3) Gultepe, E.; Nagesha, D.; Casse, B. D.; Banyal, R.; Fitchorov, T.; Karma, A.; Amiji, M.; Sridhar, S., Sustained Drug Release from Non‐Eroding Nanoporous Templates. *Small* **2010**, *6*, 213-216.

(4) Anglin, E. J.; Cheng, L.; Freeman, W. R.; Sailor, M. J., Porous Silicon in Drug Delivery Devices and Materials. *Adv. Drug Del. Rev.* **2008**, *60*, 1266-1277.

(5) Vaccari, L.; Canton, D.; Zaffaroni, N.; Villa, R.; Tormen, M.; di Fabrizio, E., Porous Silicon as Drug Carrier for Controlled Delivery of Doxorubicin Anticancer Agent. *Microelectron. Eng.* **2006**, *83*, 1598-1601.

(6) Popat, K. C.; Eltgroth, M.; LaTempa, T. J.; Grimes, C. A.; Desai, T. A., Titania Nanotubes: A Novel Platform for Drug‐Eluting Coatings for Medical Implants? *Small* **2007**, *3*, 1878-1881.

(7) Noh, K.; Brammer, K. S.; Choi, C.; Kim, S. H.; Frandsen, C. J.; Jin, S., A New Nano-Platform for Drug Release Via Nanotubular Aluminum Oxide. *J. Biomater. Nanobiotechnol.* **2011**, *2*, 226.

(8) Bianco, A.; Kostarelos, K.; Prato, M., Applications of Carbon Nanotubes in Drug Delivery. *Curr. Opin. Chem. Biol.* **2005**, *9*, 674-679.

(9) Ezzati Nazhad Dolatabadi, J.; Omidi, Y.; Losic, D., Carbon Nanotubes as an Advanced Drug and Gene Delivery Nanosystem. *Curr. Nanosci.* **2011**, *7*, 297-314.

(10) Tran, P. A.; Zhang, L.; Webster, T. J., Carbon Nanofibers and Carbon Nanotubes in Regenerative Medicine. *Adv. Drug Del. Rev.* **2009**, *61*, 1097-1114.

(11) Wood, K. C.; Chuang, H. F.; Batten, R. D.; Lynn, D. M.; Hammond, P. T., Controlling Interlayer Diffusion to Achieve Sustained, Multiagent Delivery from Layer-by-Layer Thin Films. *Proc. Natl. Acad. Sci. U. S. A.* **2006**, *103*, 10207-10212.

(12) Peppas, N. A.; Hilt, J. Z.; Khademhosseini, A.; Langer, R., Hydrogels in Biology and Medicine: From Molecular Principles to Bionanotechnology. *Adv. Mater.* **2006**, *18*, 1345.

(13) Fujita, T., Guan, P., McKenna, K., Lang, X., Hirata, A., Zhang, L., Tokunaga, T., Arai, S., Yamamoto, Y., Tanaka, N., Ishikawa, Y., Asao, N., Yamamoto, Y., Erlebacher, J. & Chen, M., Atomic Origins of the High Catalytic Activity of Nanoporous Gold. *Nat. Mater.* **2012**, *11*, 775-780.

(14) Wittstock, A.; Biener, J.; Bäumer, M., Nanoporous Gold: A New Material for Catalytic and Sensor Applications. *Phys. Chem. Chem. Phys.* **2010**, *12*, 12919-12930.

(15) Santos, G. M.; Zhao, F.; Zeng, J.; Shih, W.-C., Characterization of Nanoporous Gold Disks for Photothermal Light Harvesting and Light-Gated Molecular Release. *Nanoscale* **2014**, *6*, 5718-5724.

(16) Wittstock, A.; Neumann, B. r.; Schaefer, A.; Dumbuya, K.; Kübel, C.; Biener, M. M.; Zielasek, V.; Steinrück, H.-P.; Gottfried, J. M.; Biener, J. r., Nanoporous Au: An Unsupported Pure Gold Catalyst? *J. Phys. Chem. C* **2009**, *113*, 5593-5600.

(17) Senior, N.; Newman, R., Synthesis of Tough Nanoporous Metals by Controlled Electrolytic Dealloying. *Nanotechnology* **2006**, *17*, 2311-2316.

(18) Fujita, T.; Qian, L.; Inoke, K.; Erlebacher, J.; Chen, M., Three-Dimensional Morphology of Nanoporous Gold. *Appl. Phys. Lett.* **2008**, *92*, 251902-251904.

(19) Seker, E., Gaskins, J. T., Bart-Smith, H., Zhu, J., Reed, M. L., Zangari, G., Kelly, R. & Begley, M. R., The Effects of Post-Fabrication Annealing on the Mechanical Properties of Freestanding Nanoporous Gold Structures. *Acta Mater.* **2007**, *55*, 4593-4602.

(20) Parida, S.; Kramer, D.; Volkert, C.; Rösner, H.; Erlebacher, J.; Weissmüller, J., Volume Change During the Formation of Nanoporous Gold by Dealloying. *Phys. Rev. Lett.* **2006**, *97*, 35504-35506.

(21) Kolluri, K.; Demkowicz, M. J., Coarsening by Network Restructuring in Model Nanoporous Gold. *Acta Mater.* **2011**, *59*, 7645-7653.

(22) Erlebacher, J.; Aziz, M. J.; Karma, A.; Dimitrov, N.; Sieradzki, K., Evolution of Nanoporosity in Dealloying. *Nature* **2001**, *410*, 450-453.

(23) Ding, Y.; Kim, Y.; Erlebacher, J., Nanoporous Gold Leaf:" Ancient Technology"/Advanced Material. *Adv. Mater.* **2004**, *16*, 1897-1900.

(24) Sharma, A.; Bhattarai, J. K.; Alla, A. J.; Demchenko, A. V.; Stine, K. J., Electrochemical Annealing of Nanoporous Gold by Application of Cyclic Potential Sweeps. *Nanotechnology* **2015**, *26*, 085602.

(25) Schade, L.; Franzka, S.; Mathieu, M.; Biener, M. M.; Biener, J. r.; Hartmann, N., Photothermal Laser Microsintering of Nanoporous Gold. *Langmuir* **2014**, *30*, 7190-7197.

(26) Dorofeeva, T. S.; Seker, E., Electrically Tunable Pore Morphology in Nanoporous Gold Thin Films. *Nano Res.* **2015**, *8*, 2188-2198.

(27) Seker, E.; Reed, M. L.; Begley, M. R., Nanoporous Gold: Fabrication, Characterization, and Applications. *Materials* **2009**, *2*, 2188-2215.

(28) Shulga, O.; Zhou, D.; Demchenko, A.; Stine, K., Detection of Free Prostate Specific Antigen (Fpsa) on a Nanoporous Gold Platform. *The Analyst* **2008**, *133*, 319-322.

(29) Patel, J.; Radhakrishnan, L.; Zhao, B.; Uppalapati, B.; Daniels, R. C.; Ward, K. R.; Collinson, M. M., Electrochemical Properties of Nanostructured Porous Gold Electrodes in Biofouling Solutions. *Anal. Chem.* **2013**, *85*, 11610-11618.

(30) Daggumati, P.; Matharu, Z.; Seker, E., Effect of Nanoporous Gold Thin Film Morphology on Electrochemical DNA Sensing. *Anal. Chem.* **2015**, *87*, 8149-8156.

(31) Chapman, C. A.; Chen, H.; Stamou, M.; Biener, J.; Biener, M. M.; Lein, P. J.; Seker, E., Nanoporous Gold as a Neural Interface Coating: Effects of Topography, Surface Chemistry, and Feature Size. *ACS Appl. Mater. Inter.* **2015**, *7*, 7093-7100.

(32) Seker, E.; Berdichevsky, Y.; Begley, M.; Reed, M.; Staley, K.; Yarmush, M., The Fabrication of Low-Impedance Nanoporous Gold Multiple-Electrode Arrays for Neural Electrophysiology Studies. *Nanotechnology* **2010**, *21*, 125504.

(33) Kurtulus, O.; Daggumati, P.; Seker, E., Molecular Release from Patterned Nanoporous Gold Thin Films. *Nanoscale* **2014**, *6*, 7062 - 7071.

(34) Daggumati, P.; Kurtulus, O.; Chapman, C. A. R.; Dimlioglu, D.; Seker, E., Microfabrication of Nanoporous Gold Patterns for Cell-Material Interaction Studies. *J. Vis. Exp.* **2013**.

(35) Tan, Y. H.; Davis, J. A.; Fujikawa, K.; Ganesh, N. V.; Demchenko, A. V.; Stine, K. J., Surface Area and Pore Size Characteristics of Nanoporous Gold Subjected to Thermal, Mechanical, or Surface Modification Studied Using Gas Adsorption Isotherms, Cyclic Voltammetry, Thermogravimetric Analysis, and Scanning Electron Microscopy. *J. Mater. Chem.* **2012**, *22*, 6733-6745.

(36) Lian, H.-Y.; Liang, Y.-H.; Yamauchi, Y.; Wu, K. C.-W., A Hierarchical Study on Load/Release Kinetics of Guest Molecules into/from Mesoporous Silica Thin Films. *J. Phys. Chem. C* **2011**, *115*, 6581-6590.

(37) Liu, Z.; Sun, X.; Nakayama-Ratchford, N.; Dai, H., Supramolecular Chemistry on Water-Soluble Carbon Nanotubes for Drug Loading and Delivery. *ACS Nano* **2007**, *1*, 50-56.

(38) Huang, L.; Seker, E.; Landers, J. P.; Begley, M. R.; Utz, M., Molecular Interactions in Surface-Assembled Monolayers of Short Double-Stranded DNA. *Langmuir* **2010**, *26*, 11574-11580.

(39) Seker, E.; Reed, M.; Begley, M., A Thermal Treatment Approach to Reduce Microscale Void Formation in Blanket Nanoporous Gold Films. *Scripta Mater.* **2009**, *60*, 435-438.

(40) Nor'azim Mohd Yunos, R. B.; Story, D.; Kellum, J., Bench-to-Bedside Review: Chloride in Critical Illness. *Crit. Care* **2010**, *14*, 226.

(41) Berend, K.; van Hulsteijn, L. H.; Gans, R. O. B., Chloride: The Queen of Electrolytes? *Eur. J. Intern. Med.* **2012**, *23*, 203-211.

(42) Xue, Y.; Markmann, J.; Duan, H.; Weissmüller, J.; Huber, P., Switchable Imbibition in Nanoporous Gold. *Nat. Commun.* **2014**, *5*.

(43) Shi, Z.; Lipkowski, J., Chloride Adsorption at the Au (111) Electrode Surface. *J. Electroanal. Chem.* **1996**, *403*, 225-239.

(44) Lipkowski, J.; Shi, Z.; Chen, A.; Pettinger, B.; Bilger, C., Ionic Adsorption at the Au (111) Electrode. *Electrochim. Acta* **1998**, *43*, 2875-2888.

(45) Magnussen, O. M., Ordered Anion Adlayers on Metal Electrode Surfaces. *Chem. Rev.* **2002**, *102*, 679-726.

(46) Baker, T. A.; Friend, C. M.; Kaxiras, E., Chlorine Interaction with Defects on the Au (111) Surface: A First-Principles Theoretical Investigation. *J. Chem. Phys.* **2008**, *129*, 104702.

(47) Baker, T. A.; Friend, C. M.; Kaxiras, E., Nature of Cl Bonding on the Au (111) Surface: Evidence of a Mainly Covalent Interaction. *J. Am. Chem. Soc.* **2008**, *130*, 3720-3721.

(48) Zhang, Z.; Li, H.; Zhang, F.; Wu, Y.; Guo, Z.; Zhou, L.; Li, J., Investigation of Halide-Induced Aggregation of Au Nanoparticles into Spongelike Gold. *Langmuir* **2014**, *30*, 2648-2659.

(49) Papadopoulou, V.; Kosmidis, K.; Vlachou, M.; Macheras, P., On the Use of the Weibull Function for the Discernment of Drug Release Mechanisms. *Int. J. Pharm.* **2006**, *309*, 44-50.

(50) Bodé Jr, D. D., Calculated Free Energies of Absorption of Halide and Hydroxide Ions by Mercury, Silver, and Gold Electrodes. *J. Phys. Chem.* **1972**, *76*, 2915-2919.

(51) Almora-Barrios, N.; Novell-Leruth, G.; Whiting, P.; Liz-Marzán, L. M.; López, N. r., Theoretical Description of the Role of Halides, Silver, and Surfactants on the Structure of Gold Nanorods. *Nano Lett.* **2014**, *14*, 871-875.

(52) Dursun, A.; Pugh, D. V.; Corcoran, S. G., Dealloying of Ag-Au Alloys in Halide-Containing Electrolytes Affect on Critical Potential and Pore Size. *J. Electrochem. Soc.* **2003**, *150*, B355-B360.

(53) *Nanoporous Gold: From an Ancient Technology to a High-Tech Material*. Royal Society of Chemistry: 2012.

(54) Jeon, G.; Yang, S. Y.; Byun, J.; Kim, J. K., Electrically Actuatable Smart Nanoporous Membrane for Pulsatile Drug Release. *Nano Lett.* **2011**, *11*, 1284-1288.

(55) Aznar, E.; Marcos, M. D.; Martínez-Máñez, R. N.; Sancenón, F.; Soto, J.; Amorós, P.; Guillem, C., Ph-and Photo-Switched Release of Guest Molecules from Mesoporous Silica Supports. *J. Am. Chem. Soc.* **2009**, *131*, 6833-6843.

(56) Hoare, T.; Timko, B. P.; Santamaria, J.; Goya, G. F.; Irusta, S.; Lau, S.; Stefanescu, C. F.; Lin, D.; Langer, R.; Kohane, D. S., Magnetically Triggered Nanocomposite Membranes: A Versatile Platform for Triggered Drug Release. *Nano Lett.* **2011**, *11*, 1395-1400.

(57) Yang, X.; Liu, X.; Liu, Z.; Pu, F.; Ren, J.; Qu, X., Near‐Infrared Light‐Triggered, Targeted Drug Delivery to Cancer Cells by Aptamer Gated Nanovehicles. *Adv. Mater.* **2012**, *24*, 2890-2895.

(58) Gao, Q.; Xu, Y.; Wu, D.; Sun, Y.; Li, X., ph-Responsive Drug Release from Polymer-Coated Mesoporous Silica Spheres. *J. Phys. Chem. C* **2009**, *113*, 12753-12758.

(59) Buchsbaum, S. F.; Nguyen, G.; Howorka, S.; Siwy, Z. S., DNA-Modified Polymer Pores Allow ph-and Voltage-Gated Control of Channel Flux. *J. Am. Chem. Soc.* **2014**, *136*, 9902-9905.

(60) Marmisollé, W. A.; Capdevila, D. A.; de la Llave, E.; Williams, F. J.; Murgida, D. H., Self-Assembled Monolayers of Nh2-Terminated Thiolates: Order, Pka, and Specific Adsorption. *Langmuir* **2013**, *29*, 5351-5359.

(61) Arima, Y.; Iwata, H., Effect of Wettability and Surface Functional Groups on Protein Adsorption and Cell Adhesion Using Well-Defined Mixed Self-Assembled Monolayers. *Biomaterials* **2007**, *28*, 3074-3082.

(62) Gittard, S. D.; Pierson, B. E.; Ha, C. M.; Wu, C. A. M.; Narayan, R. J.; Robinson, D. B., Supercapacitive Transport of Pharmacologic Agents Using Nanoporous Gold Electrodes. *Biotechnol. J.* **2010**, *5*, 192-200.

(63) Pingarrón, J. M.; Yanez-Sedeno, P.; González-Cortés, A., Gold Nanoparticle-Based Electrochemical Biosensors. *Electrochim. Acta* **2008**, *53*, 5848-5866.

(64) Xie, J.; Lee, S.; Chen, X., Nanoparticle-Based Theranostic Agents. *Adv. Drug Del. Rev.* **2010**, *62*, 1064-1079.

(65) Xie, J.; Zhang, Q.; Lee, J. Y.; Wang, D. I., The Synthesis of Sers-Active Gold Nanoflower Tags for in Vivo Applications. *ACS Nano* **2008**, *2*, 2473-2480.

TABLE OF CONTENTS IMAGE